

Authors Comments

Reply to comments, Referee #1

We would like to thank Referee #1 for his/her time, constructive and helpful comments and suggestions.

1) Pg 23283, line 20 to Pg 23284 line 12: It terms of satellite validations you mention IASI, but you might also want to mention the potential for the FTIR to provide direct profile comparisons similar to recent satellite/aircraft validation studies (e.g. Shephard et al., "2015, Tropospheric Emission Spectrometer (TES) satellite validations of ammonia, methanol, formic acid, and carbon monoxide over the Canadian oil sands AMTD).

We added the following sentence as a pointer to the potential of the FTIR observations as a validation tool for nh₃-profile observations.

"A recent study by Shephard et al. (2015b) shows the potential of an instrument that can be used for profile comparisons. In the study instruments on an aircraft were used measure a vertical profile of NH₃ which were used as a validation tool for the NH₃-profile observations of TES."

Added the reference:

"Shephard, M. W., McLinden, C. A., Cady-Pereira, K. E., Luo, M., Moussa, S. G., Leithead, A., Liggio, J., Staebler, R. M., Akingunola, A., Makar, P., Lehr, P., Zhang, J., Henze, D. K., Millet, D. B., Bash, J. O., Zhu, L., Wells, K. C., Capps, S. L., Chaliyakunnel, S., Gordon, M., Hayden, K., Brook, J. R., Wolde, M., and Li, S.-M.: Tropospheric Emission Spectrometer (TES) satellite validations of ammonia, methanol, formic acid, and carbon monoxide over the Canadian oil sands, *Atmos. Meas. Tech. Discuss.*, 8, 9503-9563, doi:10.5194/amtd-8-9503-2015, 2015b."

We also changed the already included Shephard et al (2015) reference to (2015a) in the introduction (Page 23283, line 24, added 2015a (was missing)) and the reference list (Page 23302, Line 18):

"Shephard, M. W. and Cady-Pereira, K. E.: Cross-track Infrared Sounder (CrIS) satellite observations of tropospheric ammonia, *Atmos. Meas. Tech.*, 8, 1323-1336, doi:10.5194/amt-8-1323-2015, 2015b."

2) Pg 23289, lines 7-10: Can more justification be provided for there being no correlations between the layers? For example, is the vertical resolution comparable to the number of vertical retrievals levels? Looking at the averaging kernels they appear to be relatively smooth indicating that there might appear to be significant interlayer correlations.

The resolution of the retrieved profile is not the same as the number of the vertical layers. The resolution of the profile is given by the AVK. The AVK reflect the fact, that the information content in the measurement is not high enough to retrieve more than one or two independent layers in case of NH₃. From the FTIR measurements one cannot draw the conclusion, that there are interlayer correlations just because the AVK indicate this.

3) Pg 23290, lines 22-23 and Pg 23294 lines 22-23: It probably not completely accurate to say that 1 DOFS means that only total columns can be retrieved. It can be stated that with 1 DOFS only one piece of information can be obtained, but this is not necessary over the whole column unless the retrieval is equally sensitive over the whole column. For example, the retrieval might be mostly sensitive over a certain region of the profile

so the 1 DOFS might refer to more of a partial column, etc.

Changed page 23290, lines 22-23, removed “which means that only total columns can be retrieved.”
Added “with almost no vertical information available”.

Page 23294, lines 22-23, changed” only the total columns can be retrieved” to “there is not enough information to discriminate individual layers”

4) Pg. 23291, line 15-17: To reduce some of the propagation errors due to NCEP temperature uncertainties, is it possible to also perform a temperature retrieval using the CO₂ lines with or before the NH₃ retrievals? I am not proposing it is to be done here for the results in this paper, but rather just a comment (maybe in the future).

It would be possible to do this if one had a band of CO₂ in the spectral window, because you can get the temperature from the relative size of the CO₂ lines. The one line in our micro windows is not enough.

5) Pg. 23294, lines 27-29 and Pg 23295 lines 1-7: To help demonstrate the information content that goes along with the sensitivity of these low values at Jungfraujoch it would be good to also provide the average DOFS with the average retrieved values.

Added the average DOFS,

For Bremen: Page 23294, line 13, added “, with a mean DOFS 1.9”

For Jungfraujoch: Page 23294, line 14 , added” , with a mean DOFS 1.0”

6) Pg. 23295 lines 23-29 Pg. 23296 line 1: When providing background information on emission inventories you might want to also mention top-down constraints being provided by satellites (e.g. Zhu et al., 2013, Constraining U.S. ammonia emissions using TES remote sensing observations and the GEOS-Chem adjoint model, ACP), and the potential of using both FTIR and satellite observations in conjunction with chemical transport model inversions to improve emission estimates.

We’ve added a few words to point out earlier studies and use of ammonia remote sensing for emission estimate purposes:

Added “Satellite observations in combination with chemical transport models (CTM) have been used to provide a top-down constraint on ammonia emissions (e.g. Zhu et al., 2013).” In between “... the performance of air quality models (Skjoth et al., 2011).” And “Similar to satellite”.

Added to Page 23296 line 3:” and satellite” in between “,FTIR total columns in combination with surface” and “observations could provide the means to evaluate the emission”

Added “Zhu, L., Henze, D. K., Cady-Pereira, K. E., Shephard, M. W., Luo, M., Pinder, R. W., Bash, J. O. and Jeong, G. R.: Constraining U.S. ammonia emissions using TES remote sensing observations and the GEOS-Chem adjoint model, J. Geophys. Res. Atmos., 118(8), 3355–3368, doi:10.1002/jgrd.50166, 2013.” To the reference list

Edits:

1) One overall grammar correction is often there should be a “,” before the word “but”

We added a “,” to the following lines:

Page 23282, line 27,

Page 23283, line 5,

Page 23283, line 16,

Page 23284, line 15.

2) Pg 23282, line 7: missing the “a” between “is major”

Added “a”

3) Pg 23282, lines 10-12: Might want to remove “Recently” as the reference is from 2008.

Removed “Recently”

4) Pg 23282, line 28: change “and” to “with”?

Changed “and” to “with” and removed “are” from the sentence.

5) Pg 23283, line 1: might want to put brackets around the “e.g. many . . . 4 weeks”

Added brackets.

6) Pg 23283, line 22-23: missing reference for CrIS

As stated in the answer to question 1 we added the reference.

7) Pg 23284, lines 4-5: If you like you can make this statement more general by just stating that satellite data is on order the order of 10’s of kilometers.

Changed the sentence to: “whereas satellite observations have a footprint on the order of tens of kilometres.”

8) Pg 23284, line 18-19: the molecule names (e.g. Carbon Dioxide) don’t need to be capitalized in the sentence.

Removed the capital letters.

9) Pg 23285, line 12: change “and a HgCdTe” to “with a HgCdTe”

Changed to “with a HgCdTe”.

10) Pg 23288, line 15: should use “signal-to-noise ratio” for the “SNR”

Changed “SNR” to “signal-to-noise ratio”, also changed the “SNR” in the header of table 2 to “Signal-to-noise ratio (SNR)”

11) Pg 23293, line 9-11: units on the error numbers.

Added “molecules $\text{NH}_3 \text{ cm}^{-2}$ ” behind the error number.

12) Pg 23293, line 11: put a “,” before “which”

Added the “,”

Reply to comments, Referee #2

We would like to thank Referee #2 for his/her time, constructive and helpful comments and suggestions.

1) P.23283, Line 9: I prefer “artifacts” rather than “artefacts”

I kept it at “artefacts”, British versus US spelling

2) P.23283, Line 22: “CrIS” instead of “CR-IS”

Corrected as suggested

3) P.23284, Line 12: It would be better to add some more references for FTIR validation of satellite products, such as; - Wood et al., JGR, 107, 8208, doi:10.1029/2001JD000581, 2002. - Griesfeller et al., JGR, 111, D11S07, doi:10.1029/2005JD006451, 2006.

Added both references to the manuscript,

Changed line 12 to:

(Wood et al., 2002; Griesfeller et al., 2006; Dils et al., 2006; Kerzenmacher et al., 2012)

References,

Griesfeller, a., Griesfeller, J., Hase, F., Kramer, I., Loës, P., Mikuteit, S., Raffalski, U., Blumenstock, T. and Nakajima, H.: Comparison of ILAS-II and ground-based FTIR measurements of O₃, HNO₃, N₂O, and CH₄ over Kiruna, Sweden, J. Geophys. Res., 111(D11), D11S07, doi:10.1029/2005JD006451, 2006.

Wood, S. W.: Validation of version 5.20 ILAS HNO₃, CH₄, N₂O, O₃, and NO₂ using ground-based measurements at Arrival Heights and Kiruna, J. Geophys. Res., 107(D24), 8208, doi:10.1029/2001JD000581, 2002.

We also added a few extra references to earlier applications of FTIR techniques to estimate NH₃ emissions from fires,

P.23284, line 15,

Changed “by Paton-Walsh et al. (2005)” to, “from fires (Yokelson et al., 1997, 2007, Paton-Walsh et al., 2005)) but”

References:

Yokelson, R. J., Susott, R., Ward, D. E., Reardon, J. and Griffith, D. W. T.: Emissions from smoldering combustion of biomass measured by open-path Fourier transform infrared spectroscopy, J. Geophys. Res., 102(D15), 18865, doi:10.1029/97JD00852, 1997.

Yokelson, R., Urbanski, S., Atlas, E., Toohey, D., Alvarado, E., Crouse, J., Wennberg, P., Fisher, M., Wold, C., Campos, T., Adachi, K., Buseck, P. R. and Hao, W. M.: Emissions from forest fires near Mexico City, Atmos. Chem. Phys. Discuss., 7(3), 6687–6718, doi:10.5194/acpd-7-6687-2007, 2007.

4) P.23290, L.14: 1.9ĚĚ of freedom → 1.9 degree of freedom

Good one, changed to degree of freedom

5) P.23291, Line 2: DOF of 1. → DOF of 1.0.

Agreed, changed as suggested

6) P.23291, Line 24: 34.23 % for the Jungfrauoch → 34.2% for the Jungfrauoch
Corrected as suggested

7) P.23292, Line 4: Is it really “pressure and temperature broadening parameters” which are critical for the NH₃ concentrations, not “line intensity parameter”?

All three are important but the line intensity is indeed the most critical,
Changed line 4 to: Hence, line intensity parameters of the ammonia absorption lines are critical for the NH₃ concentrations.

8) P.23292, Line 11: mean column total of 13.7 → mean total column of 13.8

The number 13.75 in table 5 was rounded from the number 13.74500.
13.7 is the correct rounded value.

9) P.23293, Line 9: As for Bremen → As for Lauder

Removed “As for Bremen” for clarity

10) P.23293, Line 15: The bottom panel → The third panel

Corrected as suggested

11) P.23293, Line 17: 0.82×10^{15} → 0.80×10^{15}

Corrected as suggested

12) P.23294, Line 13: mean of 13.47 → mean of 13.8

Corrected to: 13.7, see comment 8.

13) P.23295, Line 1: I prefer “artifacts” rather than “artefacts”

I kept it at “artefacts”, British versus US spelling

14) P.23295, Line 16: NH₃ → NH₃ (subscript)

Corrected as suggested

15) P.23296, Line 9: observations at 9.30. → observations at 9:30 local time.

Corrected as suggested

1 Retrieval of ammonia from ground-based FTIR solar spectra

2

3 E. Dammers¹, C. Vigouroux², M. Palm³, E. Mahieu⁴, T. Warneke³, D. Smale⁵, B. Langerock², B. Franco⁴, M. Van
4 Damme^{1,6}, M. Schaap⁷, J. Notholt³ and J.W. Erisman^{1,8}

5 1. Cluster Earth and Climate, Department of Earth Sciences, Vrije Universiteit Amsterdam, Amsterdam, the
6 Netherlands

7 2. Belgian Institute for Space Aeronomy, Brussels, Belgium

8 3. Institut für Umweltphysik, University of Bremen, Bremen, Germany

9 4. Institute of Astrophysics and Geophysics, University of Liege, Belgium

10 5. National Institute of Water and Atmosphere, Lauder, New Zealand

11 6. Spectroscopie de l'Atmosphère, Service de Chimie Quantique et Photophysique, Université Libre de Bruxelles,
12 Brussels, Belgium

13 7. TNO Built Environment and Geosciences, Department of Air Quality and Climate, Utrecht, the Netherlands

14 8. Louis Bolk Institute, Driebergen, the Netherlands

15

16 **Abstract** We present a retrieval method for ammonia (NH₃) total columns from ground-based Fourier
17 Transform InfraRed (FTIR) observations. Observations from Bremen (53.10N, 8.85E), Lauder (45.04S,
18 169.68E), Reunion (20.9S, 55.50E) and Jungfraujoch (46.55N, 7.98E) were used to illustrate the capabilities of
19 the method. NH₃ mean total columns ranging three orders of magnitude were obtained with higher values at
20 Bremen (mean of 13.47e15 molecules cm⁻²) to the lower values at Jungfraujoch (mean of 0.18e15 molecules
21 cm⁻²). In conditions with high surface concentrations of ammonia, as in Bremen, it is possible to retrieve
22 information on the vertical gradient as two layers can be discriminated. The retrieval there is most sensitive to
23 ammonia in the planetary boundary layer, where the trace gas concentration is highest. For conditions with low
24 concentrations only the total column can be retrieved. Combining the systematic and random errors we have a
25 mean total error of 26% for all spectra measured at Bremen (Number of spectra (N) =554), 30% for all spectra
26 from Lauder (N=2412), 25% for spectra from Reunion (N=1262) and 34% for spectra measured at Jungfraujoch
27 (N=2702). The error is dominated by the systematic uncertainties in the spectroscopy parameters. Station
28 specific seasonal cycles were found to be consistent with known seasonal cycles of the dominant ammonia
29 sources in the station surroundings. The developed retrieval methodology from FTIR-instruments provides a
30 new way to obtain highly time-resolved measurements of ammonia burdens. FTIR-NH₃ observations will be
31 useful for understanding the dynamics of ammonia concentrations in the atmosphere and for satellite and model
32 validation. It will also provide additional information to constrain the global ammonia budget.

33

34

35 1. Introduction

36 Nitrogen emissions in the form of ammonia (NH_3), which largely derive from agriculture, have been associated
37 with acidification and eutrophication of soils and surface waters (Krupa, 2003; Vitousek et al., 1997), which may
38 reduce biodiversity in vulnerable ecosystems (Bobbink et al., 1998, 2010). Ammonia also reacts with nitric acid
39 and sulphuric acid to form ammonium salts, which account for a large fraction of particulate matter concentrations
40 (Schaap et al., 2004). Particulate matter is a major contributor to smog and is related to negative health impacts
41 (Pope et al., 2009). Moreover ammonium salts play an important role in the radiance balance of the Earth, thus
42 having an impact on climate change (Charlson et al., 1991, Erismann et al., 2007). ~~Recently it~~ was shown that
43 reduced nitrogen also plays a role in the fixation of carbon dioxide (CO_2) (Reay et al., 2008). Human activities
44 have increased the global emissions of reactive nitrogen (Nr) to the atmosphere (Holland et al., 1999). Current
45 global Nr emissions have been estimated to be almost four times larger compared to pre-industrial levels (Fowler
46 et al., 2013) with NH_3 emissions amounting to 49.3Tg in 2008 (EDGAR-Emission Database for Global
47 Atmospheric Research, 2011). Consequently this has led to large increases in atmospheric nitrogen deposition
48 (Rodhe et al., 2002; Dentener et al., 2006). Biomass burning was found to account for 11% of the global emission
49 budget of NH_3 (Bouwman et al., 1997). While the agricultural emissions dominate in the Northern Hemisphere,
50 biomass burning is one of the main sources of the NH_3 concentrations in the Southern Hemisphere.

51 Despite its central role in many environmental threats, little is known about the ammonia budget and its
52 distribution across the globe. Uncertainties in global and regional emission rates are large with errors of more than
53 50% (Erismann et al., 2007; Sutton et al., 2013). Ammonia concentrations have a large variability in time and
54 space, a short lifetime in the order of hours, and the lack of globally distributed observations hamper our
55 understanding. Surface observations are available, but these are not homogeneously distributed over the globe ~~and~~
56 ~~with~~ most observation sites ~~are~~ located in the Northern Hemisphere. Most sites provide data with a poor temporal
57 resolution (e.g. many observation networks use passive samplers with a sampling time of 2 or 4 weeks (Thijsse et
58 al., 1998; Puchalski et al., 2011)) whereas emission and deposition dynamics affect concentrations on the scale of
59 hours to days. Systems with higher sampling frequency such as the AMANDA, MARGA and (denuder) filter
60 packs are available, but the number of measurement networks using these instruments is limited as they are often
61 costly to operate (Erismann et al., 2001; Thomas et al., 2009; Mount et al., 2002; Hansen et al., 2003). Moreover,
62 measuring NH_3 is challenging and existing in-situ measurement techniques are often prone to sampling artefacts
63 (Bobruzki et al., 2010). Recent advances in open path remote sensing techniques, like (mini-) DOAS systems and
64 open path Quantum Cascaded Laser instruments show large potential to overcome part of these sampling issues
65 (Volten et al., 2012; Miller et al., 2014), but are still in the development stage and not widely applied yet. Another
66 aspect is the lack of vertical information, as most instruments only measure surface concentrations (Erismann et
67 al., 1998, 2007; Van Damme et al. 2014c). Some recent airborne measurements have been made (Nowak et al.,
68 2007, 2010; Leen et al., 2013), but only during dedicated campaigns with limited temporal and spatial coverage.
69 In short, it is very difficult to obtain detailed knowledge on the global ammonia budget using currently available
70 field observations.

71 Remote sensing products from atmospheric satellite sounders such as the Infrared Atmospheric Sounding
72 Interferometer (IASI), the Tropospheric Emission Spectrometer (TES) and the Cross-track Infrared Sounder (~~CR~~

73 [ISCRIS](#) (Van Damme et al., 2014a; Shephard et al., 2011; [2015a](#)) have become available and show good promise
74 to improve NH₃ concentration monitoring (Van Damme et al. 2014b; Luo et al., 2015; Whitburn et al. 2015).
75 However, these data sets are constrained by the overpass time of the satellite and the atmospheric conditions
76 (cloud coverage, thermal contrast, etc.). Moreover, the uncertainties associated to the data are relatively large,
77 which calls for a detailed evaluation of the data. A recent study (Van Damme et al., 2014c) showed a number of
78 challenges related to the validation. First, reliable hourly in-situ data is sparse. Second, when not using optimal
79 estimation satellite product as is the case for the IASI- NH₃ retrieval, one has to assume a vertical profile to link
80 surface concentrations to a column value. Third, the ground-based observations are often influenced by local
81 sources, whereas ~~the IASI satellite data are averaged satellite observations over a circular footprint with at~~
82 ~~best a diameter of 12 km footprint of the order of tens on kilometres. A recent study by Shephard et al (2015b)~~
83 ~~shows the potential of an instrument that can be used for profile comparisons. In the study instruments on an~~
84 ~~aircraft were used measure a vertical profile of NH₃ which were used as a validation tool for the NH₃-profile~~
85 ~~observations of TES.~~ Hence, a measurement methodology that would provide columnar and vertical profiles of
86 ammonia concentrations at a high temporal resolution would be highly beneficial for evaluating the merits of the
87 novel satellite products. Fourier Transform infrared spectrometry (FTIR) provides this methodology. Atmospheric
88 sounders have a long history for validation of satellite products. FTIR observations are already commonly used
89 for the validation of satellite products of among others, ~~Carbon-carbon~~ monoxide (CO), ~~Methane-methane~~ (CH₄)
90 and ~~Nitrous-nitrous Oxide-oxide~~ (N₂O) (Wood et al., 2002; Griesfeller et al., 2006; ~~Kerzenmacher et al., 2012~~; Dils
91 et al., 2006; [Kerzenmacher et al., 2012](#)).

92 FTIR spectrometry is a well-established remote sensing technique for the observation of atmospheric trace gases
93 (Rao and Weber, 1992). FTIR has so far been used to estimate ammonia emissions from fires ~~by (Yokelson et al.,~~
94 ~~1997, 2007, Paton-Walsh et al (., 2005))~~, but only on a campaign basis, not long-term monitoring. There are
95 several monitoring stations with FTIR instruments operated on a regular basis, providing long-term time series
96 for a suite of key tropospheric and stratospheric species, including Carbon Dioxide (CO₂), Carbon Monoxide (CO)
97 and Ozone (O₃). So far nobody has systematically analysed the FTIR measurements for NH₃. We have developed
98 a NH₃ retrieval strategies for four Network for detection of Atmospheric Composition Change (NDACC) FTIR
99 stations, spanning very different concentration conditions (polluted and remote sites), in order to obtain time-
100 series of NH₃ total columns and show its value for describing temporal variations.

101 First we present the measurement sites and the retrieval strategies in section 2. We describe the characteristics of
102 the retrieval in section 3.1.1 and the uncertainty budget in section 3.1.2. Section 3.2 constitutes of an interpretation
103 of the results in combination with a comparison with existing datasets of CO total columns and temperature to
104 distinguish between emission sources. We summarize the results in section 4.

105

106 **2. Measurement sites and retrieval strategies**

107

108 **2.1 Sites description**

109

Formatted: Subscript

110 Ground-based FTIR instruments measure the solar absorption spectra under cloud-free conditions by using a
111 Fourier Transform Spectrometer. These spectra can be analysed by using a line by line model (Pougatchev et al.,
112 1995; Hase et al., 2004, 2006), which models the spectroscopic absorption lines by using known parameters
113 from a spectroscopic database (e.g. HITRAN, Rothman et al., 2013) in combination with the radiative state of
114 the atmosphere, and an optimal estimation inversion scheme (Rodgers, 2000). Information on vertical
115 concentration profiles can be retrieved using the pressure broadening of the absorption lines. For the NDACC
116 network the spectral region measured is the near- to mid-infrared domain (740 to 4250 cm^{-1} , i.e. 13.5 to 2.4 μm)
117 ~~and with~~ a HgCdTe or InSb cooled detector (Zander et al., 2008) and a suite of optical filters are used to
118 optimize the signal-to-noise ratio in the complementary spectral regions. Instruments in the network are
119 routinely checked and characterized using laboratory measurements of HBr lines and the linefit software (Hase
120 et al., 1999) to assess the instrument line shape, alignment and measurement noise levels. Four NDACC stations
121 are used in our study, two in each hemisphere:

- 122 - The site of Bremen (53.10N, 8.85E) is especially suitable to measure variations in ammonia concentrations
123 as the surrounding state, Lower Saxony, which is a region with intensive agricultural activities with high and
124 temporal variable emissions (Dämmgen et al., 2005). In short, the ammonia total columns (molecules cm^{-2})
125 at Bremen are expected to reach high values compared to background stations. The Universität Bremen
126 operates a Bruker 125HR spectrometer and a solar tracker by Bruker GmbH, directly on the university
127 campus.
128
- 129 - The Jungfraujoch station (46.55N, 7.98E) is a high altitude station (3580 m.a.s.l.) located in Switzerland
130 (Zander et al., 2008). There are no large emissions sources surrounding the station itself as it is mostly located
131 in the free troposphere. At Jungfraujoch, a Bruker 120HR instrument is in operation since the early 1990s.
132 For the current study, specific for the Jungfraujoch site, we used a subset of spectra recorded during the 2004-
133 2013 time period with apparent solar zenith angles (SZA) between 70 and 85° to increase the capability to
134 retrieve the very low ammonia concentrations.
135
- 136 - The Lauder (45.04S, 169.68E) National Institute of Water and Atmospheric Research (NIWA) atmospheric
137 research station in Central Otago, New Zealand at an altitude of 370 (m.a.s.l.). Long-term operations started
138 in 1991 with a Bruker 120M (Griffith et al., 2003). This instrument was replaced with a Bruker 120HR in
139 October 2001. Ammonia emissions in the surrounding valley are mostly due to livestock grazing on the
140 pastures and a by-product of seasonal fertilizer application. In recent years there has been an increase in cattle
141 grazing and crop cultivation (EDGAR-Emission Database for Global Atmospheric Research, 2011).
142
- 143 - Reunion Island (20.9S, 55.50E) is located in the Indian Ocean to the east of Madagascar. The station is located
144 at the University campus of St.-Denis on the north side of the island. Agricultural activities are mostly related
145 to sugar cane production. The island is prone to some local biomass burning and wild fire events, which are
146 known to emit ammonia. It is also very close to Madagascar, a region with frequent and intense biomass
147 burning events, and it has been found using backward trajectory that the emissions in Madagascar can be
148 transported to Reunion Island within one day (Vigouroux et al., 2009). The measurements used in this study

149 are performed with a Bruker 120M spectrometer. Details on the measurements can be found in Senten et al.
150 (2008) and Vigouroux et al. (2012).

151
152 These stations are expected to provide significant differences in variability and levels of ammonia, making them
153 suitable to demonstrate the strength of our retrieval scheme for application across the whole network. A summary
154 of the station descriptions is given in Table 1. CO columns were obtained from the NDACC database to be used
155 for comparison in section 3.

156 2.2 NH₃ Retrieval Strategies

157
158 The ammonia absorption lines from its ν_2 vibrational band can be observed in the 700-1350 cm^{-1} wavenumber
159 range, which are also used in the retrieval of satellite products of ammonia (e.g. Clarisse et al., 2009, Van Damme
160 et al., 2014a). In this spectral range the FTIR spectra can be measured using a potassium bromide (KBr) beam-
161 splitter in combination with a mercury cadmium telluride (MCT) nitrogen cooled detector (Zander et al., 2008).
162 The retrieval scheme of trace gas concentrations from FTIR spectra is built on the use of a set of spectral micro
163 windows containing absorption lines of the targeted species, with minimum interference by other atmospheric
164 species or solar lines. Two slightly different set of spectral micro-windows were used at the four stations, but they
165 both use the same main NH₃ absorption lines. The target and interfering species are summarized in Table 2, with
166 the profile retrieved species indicated in bold. To properly estimate ammonia, interfering species like O₃ and water
167 vapour (H₂O) that overlap NH₃ lines in the ν_2 vibrational band have to be accounted for. Two micro windows
168 were chosen that contain as little interfering species as possible. In both sets, the first micro window (MW1)
169 covers the NH₃ absorption line at 930.75 cm^{-1} . At Bremen/Lauder, the choice was to use only isolated NH₃
170 absorption features to avoid possible problems due to line mixing, therefore the spectral window MW1 is only 1
171 cm^{-1} wide [930.32-931.32, MW1]. Figure 1 shows an example of a synthetic spectrum calculated to fit a
172 observation that was measured with the 125HR in Bremen on the 19th of April 2010 at 09:59 (UTC) (Solar Zenith
173 Angle of 45 degrees). The NH₃ concentrations on this day were slightly higher than average resulting in slightly
174 stronger NH₃ absorption features in the spectra. The top two figures show the absorption contributions of the
175 absorbing species in both micro windows. The bottom two panels show an enlarged version of the figure to
176 distinguish the interfering species with smaller absorption features. At Reunion Island/Jungfrauoch, MW1 was
177 extended [929.4-931.4, MW1] to cover another NH₃ line at 929.9 cm^{-1} . This improved the retrieval for Reunion
178 Island because at this location the NH₃ concentration levels are much lower than at Bremen and the water vapour
179 concentrations are much higher. In this high humidity condition, the 930.75 cm^{-1} line is not isolated from H₂O,
180 and it improved the retrieval to add the more isolated one at 929.9 cm^{-1} (see Figure 2). The main interfering species
181 in MW1 are CO₂, N₂O, and H₂O. Minor interfering species are SF₆ and CFC-12. The second window is spanning
182 the NH₃ line at 967.35 cm^{-1} . Again, different widths are used for Bremen/Lauder [966.97-967.68, MW2] and
183 Reunion Island/Jungfrauoch [962.7-970, MW2]. The very weak absorption signatures at Reunion Island and
184 Jungfrauoch are close to the noise level and therefore the whole NH₃ absorption shape is retrieved (about 964-
185 968 cm^{-1} , see Figure 2) rather than a single line. The main interfering species in MW2 are O₃, CO₂ and H₂O for
186 all sites. At Reunion Island HDO is also interfering in MW2 as well as the isotopologue ⁶⁸⁶O₃ (i.e. ¹⁶O-¹⁸O-¹⁶O),
187 which has been fitted in addition to the main ⁶⁶⁶O₃. At Jungfrauoch apart from CO₂, two O₃ isotopologues (the

189 most abundant and ⁶⁸⁶ O₃) and water vapour which are the main interferences, N₂O, CFC-12, SF₆ and HDO
190 absorptions are also retrieved. Typical NH₃ absorptions are weak, on the order of a few tenths of a percent. The
191 typical measurement noise (**SNR_{signal-to-noise ratio}**) differs per spectra and site but ranges between ~250 at
192 Lauder to ~450 at Bremen. Channelling was not an issue in any of the spectra and did not need to be fitted.

193
194 Except at Jungfraujoch where SFIT2 is used, the retrieval is performed using the more recent SFIT4.0.9.4
195 algorithm (Pougatchev et al., 1995, Hase et al., 2004, 2006). Both versions use a form of the optimal estimation
196 method (Rodgers et al., 2000) to retrieve the volume mixing ratios and total columns of NH₃ and makes use of
197 a-priori information (profile and covariance matrix). For Bremen, Lauder and Jungfraujoch the used NH₃ a-
198 priori volume mixing ratios are based on balloon observations (Toon et al. 1999, NH₃ available in dataset but
199 not reported). The shape of the balloon measurements profile was kept constant but extended and scaled to
200 expected surface concentrations. The a-priori surface volume mixing ratio is estimated to be 10 ppb for Bremen
201 (Dämmgen et al., 2005). Although the shape of NH₃ profiles do change through time, the largest share of NH₃ is
202 expected to be in the mixing layer, which is represented by the lowest layers in the calculation (Van Damme et
203 al 2014c, Nowak et al., 2010). At Reunion Island, the a priori profile was taken from the MOZART model
204 (Louisa Emmons, private communication). The a-priori profile peaks at a higher altitude (4-5 km) instead of the
205 boundary layer as in Bremen, as NH₃ is expected to originate mainly from transport of biomass burning
206 emissions at this location. At all stations, the a-priori profiles of the interfering species were taken from the
207 Whole Atmosphere Community Climate Model (Chang et al., 2008).

208
209 At Bremen and Lauder, the a priori covariance matrices only have diagonal values corresponding to standard
210 deviations of 100% for all layers with no interlayer correlation, chosen in relation to the large range of possible
211 concentrations and variations between layers. At Jungfraujoch and Reunion Island, we did not use the a priori
212 covariance matrix as in optimal estimation but the Tikhonov type L₁ regularization (e.g. Sussmann et al., 2009)
213 was adopted for the Jungfraujoch retrievals. After several tests, values of 50 and 250 were adopted for the alpha
214 parameter and the signal to noise for inversion, respectively. A Tikhonov regularization with an alpha parameter
215 value of 50 was also adopted for the Reunion retrievals. The signal to noise ratio is calculated for each spectra,
216 the mean value being 365.

217
218 Daily temperature and pressure profiles for the meteorological variables were taken from NCEP (National
219 Center for Environment Prediction). For the radiative transfer calculations the profiles were split into about 50
220 levels, depending slightly on the station, from ground up to 80 kilometres (100 kilometres in the case of
221 Jungfraujoch and Reunion Island). The layers have a typical thickness of 500 meters in the troposphere up to 2
222 km for the higher layers. For the line spectroscopy we use the HITRAN 2012 database (Rothman et al., 2013) in
223 combination with a number of corrections for CO₂ (ATMOS, Brown et al., 1996) (except for Jungfraujoch for
224 which the HITRAN lines are used) and sets of pseudo lines generated by G.C. Toon (NASA-JPL) to account for
225 broad unresolved absorptions by heavy molecules (e.g. CFC-12, SF₆).

226
227 Figure 3 shows an example of the fit in both micro windows for the same measured spectra as used in Figure 1.
228 The top two and bottom two panels show the calculated (Green line) and measured spectrum (Blue line) and the

229 residual of both micro windows. The simultaneous fits are good with a standard deviation of 0.15% in both
230 cases.
231

232 **3. Results of the FTIR retrievals**

233 **3.1 Characteristics of the NH₃ retrievals**

234 **3.1.1 Vertical Information**

235 The retrieved vertical information differs from station to station. The top of Figure 4 shows for the 4 stations the
236 average NH₃ volume mixing ratios (VMR) for each of the retrieved layers (blue line) and the a priori profile that
237 was used as input in the retrieval (green line). The bottom of Figure 4 shows the averaging kernels for each of the
238 4 stations averaged over all available observations. As mentioned earlier most of the NH₃ at Bremen is in the
239 lowest layers. In Figure 4 this is also observed as the averaging kernel shows the most sensitivity in the lowest
240 layers (red and green lines for the layers 0.03-0.5km and 0.5-1km). The combination of the two spectral micro
241 windows on average contain 1.9 degrees of freedom for signal (DOFS) for the Bremen spectra, which means
242 around two independent vertical layers can be retrieved. The two separate layers consist of a layer covering
243 ground-1km and one that covers 1 km - 6 km height, which can be observed in Figure 4. It must be taken into
244 account however that the shown averaging kernels are a mean for all observations and thus the retrievable number
245 of layers and combined layer depths vary from spectra to spectra. On average, the Lauder spectra have a DOFS
246 of 1.4. There is only vertical information for multiple layers during periods with increased NH₃ total columns,
247 which mostly occur during summer. Similar to Bremen averaging kernels peak near the surface. At Reunion Island
248 only 1.0 DOFS is achieved, ~~which means that only total columns can be retrieved with almost no vertical~~
249 ~~information available~~. All the averaging kernels are peaking at the same altitude (about 5km), which is also the
250 peak of the a priori profile (Figure 4). Similar to the Reunion spectra the Jungfraujoch spectra do not have vertical
251 information with a DOF of 1.0.

252
253 **3.1.2 Uncertainties Budget**

254 For the error analysis the posteriori error calculation included in the SFIT4 package is used. The error calculation
255 is based on the error estimation approach by Rodgers (2000). It allows the calculation of the error by attributing
256 errors to each of the parameters used in the retrieval. The error budget can be divided into three contributions, the
257 error due to the forward model parameters, the measurement noise and the error due to the vertical resolution of
258 the retrieval (smoothing error). The assumed uncertainties for the used parameters in the retrieval are listed in
259 Table 3 for the parameters used in the calculation for Bremen, Lauder and Reunion. For Jungfraujoch, the error
260 computation was performed using the perturbation method, the spectra of 2009 to 2011 and the Rodger formalism
261 as explained e.g. in Franco et al., 2015. For Reunion Island, the covariance matrix used for the smoothing error
262 has diagonal elements representing 150% of variability from the a priori profile. To reflect the error in the NCEP
263 temperature profiles we assume an uncertainty of about 2 K in the troposphere and a 5 K uncertainty in the
264 stratosphere. For the uncertainty in the NH₃ line parameters we assume values as stated in the HITRAN 2012
265 database. We assume a conservative 20% uncertainty for the intensity and 10% for both the temperature and
266 pressure broadening coefficients.

267
268 The results of the error calculation are listed in in Table 4. Combining the systematic and random errors we have
269 a mean total error of 25.8 % for all the spectra measured at Bremen (N=554), 30.2 % for the spectra from Lauder
270 (N=2412), 25.2 % for the Reunion spectra (N=1262) and 34.23-2 for the Jungfraujoch spectra (N=2702). The
271 errors are dominated by uncertainties in the spectroscopy. In detail, the random error sources amount to a mean

272 error of 9.1 % for the Bremen spectra, which is mostly due to uncertainty in temperature, measurement noise and
273 the zero level of the sensor (i.e. an instrument property). In the case of the systematic error, with a mean error of
274 23.5 %, the error is for the largest part due to the spectroscopy (i.e. line parameters) with smaller contributions of
275 the temperature, zero level, phase and the smoothing error. The results are similar for the Lauder, Reunion and
276 Jungfraujoch spectra with most of the uncertainty coming from the line parameters. Hence, line intensity
277 ~~parameters~~the pressure and temperature broadening parameters of the ammonia absorption lines are critical for
278 the NH₃ concentrations.

279

280 3.2 Time series

281 Figure 5 shows the NH₃ total columns retrieved from all available spectra from 2004-2013. Table 5 gives a
282 summary of statistics of the retrieved NH₃ columns. Individual measurements at Bremen (blue) show high
283 concentrations, especially in spring with an overall mean column total of 13.7e15 molecules NH₃ cm⁻² and a root
284 mean square (RMS) of 20.22 indicating a large variability in the observations. The amplitude of the spring peaks
285 vary throughout the years, with maxima in 2010 and 2013 reaching ~93e15 and 85e15 molecules NH₃ cm⁻². The
286 variability through the years is caused by changes in meteorology, emissions and timing of the measurements.
287 Gaps in the data are due to days with overcast and instrument downtimes. The individual observed columns are
288 sorted into monthly averages to analyse the seasonal variability and to understand the processes driving the NH₃
289 concentrations. This is shown in Figure 6 together with monthly averages of surface temperature and CO total
290 columns. NH₃ column total concentrations at Bremen (Blue line) have a seasonal cycle with highest levels during
291 spring, the summer months and autumn. The maximum concentrations occur around April which is consistent
292 with temporal emission patterns for manure application reported for this region (Friedrich and Reis, 2004; Martin
293 et al., 2015; Paulot et al., 2014). The baseline variability with higher concentrations in summer can be explained
294 by an increase in volatilization rates of NH₃, emitted from livestock housing, which is driven by animal activity
295 and temperature (Gyldenkaerne et al., 2005). A comparison with CO is made to distinguish between agricultural
296 and fire emissions sources. A correlation between NH₃ and CO columns is not observed, which is consistent with
297 agriculture as the dominant source of ammonia.

298

299 On average the measurements at Lauder (Figure 5, red line, top panel) yield a column total of 4.17e15 molecules
300 NH₃ cm⁻². These levels are about 1/3rd of the concentrations measured at Bremen (blue, top panel). Spectra from
301 Lauder are available for most days in the retrieved time series, which makes it easier to discern peaks and
302 variability. Distinctive peaks are only visible in the summers. Maxima during spring times are not often observed.
303 The peak values are similar in between years, with maxima typically around 30e15 molecules NH₃ cm⁻². ~~As for~~
304 ~~Bremen~~ The RMS of 5.95 reflects a large variability in the observations between individual retrievals. The
305 average error is 1.34e15 molecules NH₃ cm⁻², which is around a quarter of the mean. Figure 6 shows the seasonal
306 cycle of Lauder (red line, top left panel). The seasonal variation of NH₃ coincides with that of the atmospheric
307 temperature (red line, bottom right panel) and with the livestock emissions in the surrounding region, which are
308 strongly correlated with temperature.

309

310 The ~~bottom-third~~ panel of Figure 5 shows the observations from Reunion (green symbols, bottom panel). The
311 mean column total observed at Reunion is 0.82e15 80e15 molecules NH₃ cm⁻². The concentrations are low during

312 most of the year. However, peaks reaching densities of $\sim 6 \times 10^{15}$ molecules $\text{NH}_3 \text{ cm}^{-2}$ can be observed during the
313 end of each year. The peaks in September-November coincide with the dry season indicating that emissions are
314 mostly due to biomass burning and large fire events (Vigouroux et al., 2012). This is supported by the increased
315 CO concentrations, which are also observed in October and November (see, bottom left panel, Figure 6). NH_3
316 surface concentration measurements are not available for this region but a recent paper by Van Damme et al.
317 (2015), which uses IASI- NH_3 observations, shows similar seasonal cycles for the south eastern parts of Africa
318 (Madagascar). Temperature is almost constant throughout the year and not a major factor in the seasonality of
319 Reunion.

320
321 Observations from Jungfraujoch have the lowest mean concentration of all four stations (Figure 5, orange line),
322 with a mean of 0.18×10^{15} molecules $\text{NH}_3 \text{ cm}^{-2}$. The low concentrations at Jungfraujoch are expected, as the station
323 is located in the free troposphere high above the surrounding valleys. Transport of NH_3 from the valleys only
324 occurs sporadically during days with intense vertical mixing. This was also observed in an earlier study of CO
325 concentrations (Barret et al., 2003). The Jungfraujoch observations show almost no seasonal effects with only a
326 minimal increase during the summer months. The low concentrations measured at Jungfraujoch support our
327 assumption on the vertical distribution of the ammonia concentrations with low values in the troposphere that
328 were used in our a-priori.

329

330 4. Conclusions and perspectives

331

332 In this study we presented a new method to retrieve ammonia total columns from ground-based FTIR solar spectra.
333 Observations from four complementary stations were used to illustrate the capabilities of the retrieval method.
334 NH_3 total columns ranging three orders of magnitude were obtained with high abundances at Bremen (mean of
335 13.47×10^{15} molecules cm^{-2} , with a mean DOFS 1.9) to low columns at Jungfraujoch (mean of 0.18×10^{15}
336 molecules cm^{-2} , with a mean DOFS 1.0). The very low levels obtained at the Jungfraujoch demonstrate the
337 sensitivity of the retrieval method we developed. A separate error calculation shows random errors in the order of
338 10% and systematic errors of 25% for individual observations. The errors are dominated by uncertainties in
339 spectroscopy, atmospheric temperature and deviations in instrumental parameters. For conditions with high
340 surface concentrations of ammonia, as in Bremen, it is possible to retrieve information on the vertical gradient as
341 two layers can be discriminated. At Bremen, the retrieval there is most sensitive to ammonia in the planetary
342 boundary layer, where most of the ammonia is expected. For conditions with lower concentrations ~~only the total~~
343 ~~columns can be retrieved~~ there is not enough information to discriminate individual layers. Station specific
344 seasonal cycles were found to be consistent with known seasonal cycles of the dominant ammonia sources in the
345 station surroundings. For example, highest levels in Bremen were observed during spring time when manure is
346 applied to the fields with column total concentrations reaching up to 93×10^{15} molecules cm^{-2} .

347 Remote sensing techniques avoid sampling artefacts common to other techniques such as filter packs (Puchalski
348 et al., 2011; Bobruzki et al., 2010). For in-situ observations open path remote sensing techniques, e.g. DOAS and
349 QCL instruments, are starting to be used (Volten et al., 2010, Miller et al., 2014). The FTIR- NH_3 observations
350 would be an excellent addition to these approaches as it provides the NH_3 total column and profiles, including
351 vertical information for sites sampling high ammonia levels. With a mean error of $\sim 25\%$ for all observations in

352 high ammonia source areas the accuracy of the FTIR retrievals is comparable to that reported for satellite products
353 (TES, IASI, CrIS). Compared to the in-situ open path remote sensing methods the FTIR method has a higher
354 uncertainty, but this is a trade-off for the ability to retrieve vertical information. To improve the accuracy of the
355 FTIR-NH₃ retrieval a reassessment of the spectral line parameters is necessary.

356 Observations from existing networks commonly represent daily or even monthly averaged concentration values,
357 which severely complicates any attempt to validate satellite observations. The novel FTIR-NH₃ observations
358 enable a direct validation of satellite products. As the FTIR-~~NH₃~~NH₃ product provides averaging kernels a direct
359 comparison can be made with optimal estimation satellite retrievals while taking account of the a-priori
360 information and vertical sensitivity of both instruments (Rogers and Connor, 2003). A dedicated field campaign
361 was executed at the Cabauw Experimental Site for Atmospheric Remote Sensing (CESAR) in the Netherlands
362 (spring and summer 2014) to validate the IASI- NH₃ using a range of instruments including mini-DOAS
363 instruments and a Bruker IFS-66 instrument (Dammers et al. in prep).

364 The uncertainty in the emission distributions hampers the performance and prediction capabilities of air quality
365 and climate models (Heald et al., 2012). Emissions are usually based on nationally reported yearly emission
366 inventories (Pouliot et al., 2012) and gridded by distributing the emissions following animal numbers and
367 agricultural land use (Bouwman et al., 2002, Keunen et al., 2011). To improve on static emission time profiles, a
368 new direction is to include the impact of meteorological variability of ammonia emissions in modelling systems
369 (Sutton et al., 2013). Recently, such an improvement was shown to greatly enhance the performance of air quality
370 models (Skjoth et al., 2011). [Satellite observations in combination with chemical transport models \(CTM\) have](#)
371 [been used to provide a top-down constraint on ammonia emissions \(e.g. Zhu et al., 2013\).](#) Similar to satellite
372 observations, FTIR total columns in combination with surface [and satellite](#) observations could provide the means
373 to evaluate the emission modelling through comparing trends and concentration anomalies within and between
374 years. For this purpose continuous time series are necessary. Due to the lack of continuous data (i.e. more than
375 one observation per hour) we could not derive a typical diurnal cycle in this study, whereas this would be highly
376 useful for model evaluation. Improved knowledge on the diurnal cycles may also greatly help to interpret model
377 evaluation results against satellite data as they provide snapshots, e.g. daily IASI's observations at 9:30 [local](#)
378 [time](#). Also, the model-measurement comparison would be less sensitive to modelling errors in the turbulent
379 vertical exchange as the ammonia is integrated over vertical.

380 The developed retrieval methodology from FTIR-instruments provides a new way to obtain vertically and
381 temporally resolved measurements on ammonia concentrations. FTIR-NH₃ observations may prove very valuable
382 for satellite and model validation and may provide a complementary source of information to constrain the global
383 ammonia budget.

384 **Acknowledgements**

385 This work is part of the research programme GO/12-36, which is financed by the Netherlands Organisation for
386 Scientific Research (NWO). Acknowledgements are addressed to the Université de La Réunion and CNRS
387 (LACy-UMR8105 and UMS3365) for their strong support of the OPAR station (Observatoire de Physique de
388 l'Atmosphère de la Réunion) and the OSU-R (Observatoire des Sciences de l'Univers de la Réunion)

389 activities. The authors gratefully acknowledge C. Hermans and F. Scolas from BIRA-IASB, and J.-M. Metzger
390 from Université de La Réunion, for the Reunion Island measurements. We are also grateful to Louisa Emmons
391 (NCAR) who provided NH₃ profiles from the MOZART model used as a priori in the Reunion Island retrievals.
392 The University of Liège contribution to the present work has mainly been supported by the A3C project (PRODEX
393 Program of the Belgian Science Policy Office, BELSPO, Brussels). Additional support was provided by
394 MeteoSwiss (Global Atmospheric Watch), the Fédération Wallonie-Bruxelles and the F.R.S. – FNRS. We thank
395 the International Foundation High Altitude Research Stations Jungfraujoch and Gornergrat (HFSJG, Bern). E.
396 Mahieu is Research Associate with F.R.S. – FNRS. The Lauder NIWA FTIR program is funded through the New
397 Zealand Government's core research grant framework. We are grateful to the many colleagues who have
398 contributed to FTIR data acquisition at the various sites.

399

400 **References**

401

402 Barret, B., De Mazière, M., and Mahieu, E.: Ground-based FTIR measurements of CO from the Jungfraujoch:
403 characterisation and comparison with in situ surface and MOPITT data, *Atmos. Chem. Phys.*, 3, 2217-2223,
404 doi:10.5194/acp-3-2217-2003, 2003.

405

406 Bobbink, R., Hornung, M., & Roelofs, J. G. (1998). The effects of air-borne nitrogen pollutants on species
407 diversity in natural and semi-natural European vegetation. *Journal of Ecology*, 86(5), 717-738.

408

409 Bobbink, R, Hicks K, Galloway J, Spranger T, Alkemade R, Ashmore M, Bustamante M, Cinderby S, Davidson
410 E, Dentener F, Emmett B, Erisman JW, Fenn M, Gilliam F, Nordin A, Pardo L, De Vries W. Global assessment
411 of nitrogen deposition effects on terrestrial plant diversity: a synthesis, *Ecological Applications*, 20 (2010), pp.
412 30–59

413

414 von Bobruzki, K., Braban, C. F., Famulari, D., Jones, S. K., Blackall, T., Smith, T. E. L., Blom, M., Coe, H.,
415 Gallagher, M., Ghalaieny, M., McGillen, M. R., Percival, C. J., Whitehead, J. D., Ellis, R., Murphy, J.,
416 Mohacsi, A., Pogany, A., Junninen, H., Rantanen, S., Sutton, M. A., and Nemitz, E.: Field inter-comparison of
417 eleven atmospheric ammonia measurement techniques, *Atmos. Meas. Tech.*, 3, 91-112, doi:10.5194/amt-3-91-
418 2010, 2010.

419 Bouwman, A. F., Lee, D. S., Asman, W. A. H., Dentener, F. J., Van Der Hoek, K. W., & Olivier, J. G. J. (1997).
420 A global high-resolution emission inventory for ammonia. *Global biogeochemical cycles*, 11(4), 561-587.

Formatted: Dutch (Netherlands)

421 Bouwman, A. F., L. J. M. Boumans, and N. H. Batjes (2002), Estimation of global NH₃ volatilization loss from
422 synthetic fertilizers and animal manure applied to arable lands and grasslands, *Global Biogeochem. Cycles*, 16(2),
423 1024, doi:10.1029/2000GB001389.

424 Brown, L. R., M. R. Gunson, R. A. Toth, F. W. Irion, C. P. Rinsland, and A. Goldman. "1995 atmospheric trace
425 molecule spectroscopy (ATMOS) linelist." *Applied optics* 35, no. 16 (1996): 2828-2848.

426 Chang, L., Palo, S., Hagan, M., Richter, J., Garcia, R., Riggin, D. and Fritts, D.: Structure of the migrating diurnal
427 tide in the Whole Atmosphere Community Climate Model (WACCM), *Advances in Space Research*, 41(9), 1398–
428 1407, doi:10.1016/j.asr.2007.03.035, 2008.

429 Charlson, R. J., Langner, J., Rodhe, H., Leovy, C. B., and Warren, S. G.: Perturbation of the Northern-Hemisphere
430 radiative balance by backscattering from anthropogenic sulfate 15 aerosols, *Tellus A*, 43, 152–163, 1991.

431 Clarisse, Lieven, Cathy Clerbaux, Frank Dentener, Daniel Hurtmans, and Pierre-François Coheur. "Global
432 ammonia distribution derived from infrared satellite observations." *Nature Geoscience* 2, no. 7 (2009): 479-483.

433 Dämmgen, U., & Erisman, J. W. (2005). Emission, transmission, deposition and environmental effects of
434 ammonia from agricultural sources. *Kuczynski, T.; Dämmgen, U.; Webb, J.*, 97-112.

435 Dentener, F., Drevet, J., Lamarque, J. F., Bey, I., Eickhout, B., Fiore, A. M., et al. (2006). Nitrogen and sulfur
436 deposition on regional and global scales: A multimodel evaluation. *Global Biogeochemical Cycles*, 20: GB4003.
437 doi:10.1029/2005GB002672.

Formatted: English (United States)

438 Dils, B., De Mazière, M., Müller, J. F., Blumenstock, T., Buchwitz, M., de Beek, R., Demoulin, P., Duchatelet, P.,
439 Fast, H., Frankenberg, C., Gloudemans, A., Griffith, D., Jones, N., Kerzenmacher, T., Kramer, I., Mahieu, E.,
440 Mellqvist, J., Mittermeier, R. L., Notholt, J., Rinsland, C. P., Schrijver, H., Smale, D., Strandberg, A.,
441 Straume, A. G., Stremme, W., Strong, K., Sussmann, R., Taylor, J., van den Broek, M., Velasco, V., Wagner, T.,
442 Warneke, T., Wiacek, A., and Wood, S.: Comparisons between SCIAMACHY and ground-based FTIR data for
443 total columns of CO, CH₄, CO₂ and N₂O, *Atmos. Chem. Phys.*, 6, 1953-1976, doi:10.5194/acp-6-1953-2006,
444 2006.

445 EDGAR-Emission Database for Global Atmospheric Research: Source: EC-JRC/PBL. EDGAR version 4.2.,
446 <http://edgar.jrc.ec.europa.eu>, access 15th October 2012, 2011

447
448 Erisman, J. W., Vermetten, A. W., Asman, W. A., Waijers-Ijpelaar, A., & Slanina, J. (1988). Vertical distribution
449 of gases and aerosols: the behaviour of ammonia and related components in the lower atmosphere. *Atmospheric*
450 *Environment* (1967), 22(6), 1153-1160.

451 Erisman, J. W., Otjes, R., Hensen, A., Jongejan, P., van den Bulk, P., Khlystov, A., Mols, H., and Slanina, J.:
452 Instrument development and application in studies and monitoring of ambient ammonia, *Atmos. Environ.*, 35,
453 1913-1922, 2001.

454 Erisman, J. W., Bleeker, A., Galloway, J., & Sutton, M. S. (2007). Reduced nitrogen in ecology and the
455 environment. *Environmental Pollution*, 150(1), 140-149.

456 Fowler, D., Coyle, M., Skiba, U., Sutton, M. A., Cape, J. N., Reis, S., Sheppard, L. J., Jenkins, A., Grizzetti, B.,
457 Galloway, J. ., Vitousek, P., Leach, A., Bouwman, A. F., Butterbach-Bahl, K., Dentener, F., Stevenson, D.,
458 Amann, M., and Voss, M.: The global nitrogen cycle in the twenty-first century, *Philos. Trans. R. Soc. London*,
459 Ser. B, 368, Doi:10.1098/rstb.2013.0164, 2013.

460
461 Franco, B., Hendrick, F., Van Roozendaal, M., Müller, J.-F., Stavrakou, T., Marais, E. A., Bovy, B., Bader, W.,
462 Fayt, C., Hermans, C., Lejeune, B., Pinardi, G., Servais, C. and Mahieu, E.: Retrievals of formaldehyde from
463 ground-based FTIR and MAX-DOAS observations at the Jungfraujoch station and comparisons with GEOS-
464 Chem and IMAGES model simulations, *Atmospheric Measurement Techniques*, 8(4), 1733-1756,
465 doi:10.5194/amt-8-1733-2015, 2015.

466 Friedrich, R., & Reis, S. (Eds.). (2004). *Emissions of air pollutants*. Springer Science & Business Media.

467
468
469 Gyldenkerne, S., Ambelas Skjøth, C., Hertel, O., & Ellermann, T. (2005). A dynamical ammonia emission
470 parameterization for use in air pollution models. *Journal of Geophysical Research: Atmospheres* (1984-
471 2012), 110(D7).

Formatted: English (United States)

472
473 Griffith, D. W. T., Jones, N. B., McNamara, B., Walsh, C. P., Bell, W., and Bernardo, C.: Intercomparison of
474 NDSC ground-based solar FTIR measurements of atmospheric gases at Lauder, New Zealand, *J. Atmos. Ocean.*
475 *Tech.*, 20, 1138-1153, 2003.

476
477 [Griesfeller, a., Griesfeller, J., Hase, F., Kramer, I., Loës, P., Mikuteit, S., Raffalski, U., Blumenstock, T. and](#)
478 [Nakajima, H.: Comparison of ILAS-II and ground-based FTIR measurements of O₃, HNO₃, N₂O, and CH₄](#)
479 [over Kiruna, Sweden, *J. Geophys. Res.*, 111\(D11\), D11S07, doi:10.1029/2005JD006451, 2006.](#)

480
481 Hansen, D. A., E. S. Edgerton, B. E. Hartsell, J. J. Jansen, N. Kandasamy, G. M. Hidy, and C. L. Blanchard (2003),
482 The southeastern aerosol research and characterization study: Part 1. Overview, *J. Air Waste Manage. Assoc.*, 53,
483 1460-1471, doi:10.1080/10473289.2003.10466318.

484
485 Hase, F.; Blumenstock, T. & Paton-Walsh, C. Analysis of the instrumental line shape of high-resolution Fourier
486 transform IR spectrometers with gas cell measurements and new retrieval software *Appl. Opt.*, 1999, 38

487 Hase, F., et al. "Intercomparison of retrieval codes used for the analysis of high-resolution, ground-based FTIR
488 measurements." *Journal of Quantitative Spectroscopy and Radiative Transfer* 87.1 (2004): 25-52.

489

490 Hase, F., Demoulin, P., Sauval, A. J., Toon, G. C., Bernath, P. F., Goldman, A., Hannigan, J. W., Rinsland, C. P.:
491 An empirical line-by-line model for the infrared solar transmittance spectrum from 700 to 5000 cm⁻¹, *J. Quant.*
492 *Spectrosc. Ra.*, 102, 450–463, doi:10.1016/j.jqsrt.2006.02.026, 2006.

493
494 Heald, C. L., Jr., J. L. C., Lee, T., Benedict, K. B., Schwandner, F. M., Li, Y., Clarisse, L., Hurtmans, D. R.,
495 Van Damme, M., Clerbaux, C., Coheur, P.-F., Philip, S., Martin, R. V., and Pye, H. O. T.: Atmospheric
496 ammonia and particulate inorganic nitrogen over the United States, *Atmos. Chem. Phys.*, 12, 10 295–10 312,
497 doi:10.5194/acp-12-10295-2012, 2012.

498
499 Holland, E. A., Dentener, F. J., Braswell, B. H., & Sulzman, J. M. (1999). Contemporary and pre-industrial global
500 reactive nitrogen budgets. In *New Perspectives on Nitrogen Cycling in the Temperate and Tropical Americas* (pp.
501 7-43). Springer Netherlands.

502
503 Kerzenmacher, T., Dils, B., Kumps, N., Blumenstock, T., Clerbaux, C., Coheur, P.-F., Demoulin, P., García, O.,
504 George, M., Griffith, D. W. T., Hase, F., Hadji-Lazaro, J., Hurtmans, D., Jones, N., Mahieu, E., Notholt, J., Paton-
505 Walsh, C., Raffalski, U., Ridder, T., Schneider, M., Servais, C., and De Mazière, M.: Validation of IASI FORLI
506 carbon monoxide retrievals using FTIR data from NDACC, *Atmos. Meas. Tech.*, 5, 2751-2761, doi:10.5194/amt-
507 5-2751-2012, 2012.

508
509 Kuenen, J., H. Denier van der Gon, A. Visschedijk, H. van der Brugh, and R. van Gijlswijk (2011), MACC
510 European emission inventory for the years 2003–2007, *TNO Rep. TNO-060-UT-2011-00588*, TNO, Utrecht,
511 Netherlands.

512
513 Mount, G. H., Rumburg, B., Havig, J., Lamb, B., Westberg, H., Yonge, D., Johnson, K., and Kincaid, R.:
514 Measurement of atmospheric ammonia at a dairy using differential optical absorption spectroscopy in the mid-
515 ultraviolet, *Atmos. Environ.*, 36, 1799–1810, 2002.

516
517 Krupa, S.: Effects of atmospheric ammonia (NH₃) on terrestrial vegetation: a review, *Environ. Pollut.*, 124, 179
518 – 221, doi:http://dx.doi.org/10.1016/S0269-7491(02)00434-7, 2003.

519
520 Leen, J. B., Yu, X. Y., Gupta, M., Baer, D. S., Hubbe, J. M., Kluzek, C. D., ... & Hubbell, M. R. (2013). Fast In
521 Situ Airborne Measurement of Ammonia Using a Mid-Infrared Off-Axis ICOS Spectrometer. *Environmental*
522 *science & technology*, 47(18), 10446-10453.

523
524 Luo, M., Shephard, M. W., Cady-Pereira, K. E., Henze, D. K., Zhu, L., Bash, J. O., Pinder, R. W., Capps, S., and
525 Walker, J.: Satellite Observations of Tropospheric Ammonia and Carbon Monoxide: Global Distributions,
526 Correlations and Comparisons to Model Simulations, *Atmos. Environ.*, 106, 262–277,
527 doi:10.1016/j.atmosenv.2015.02.007, 2015

528
529 Miller, D. J., Sun, K., Tao, L., Khan, M. A., and Zondlo, M. A.: Open-path, quantum cascade-laser-based sensor
530 for high-resolution atmospheric ammonia measurements, *Atmos. Meas. Tech.*, 7, 81-93, doi:10.5194/amt-7-81-
531 2014, 2014.

532
533 Mount G H, Rumburg B, Havig J, Lamb B, Westberg H, Yonge D, Johnson K and Kincaid R 2002 Measurement
534 of atmospheric ammonia at a dairy using differential optical absorption spectroscopy in the mid-ultraviolet *Atmos.*
535 *Environ.* 36 1799–810

536
537 Nowak, J. B., Neuman, J. A., Kozai, K., Huey, L. G., Tanner, D. J., Holloway, J. S., Ryerson, T. B., Frost, G. J.,
538 McKeen, S. A., and Fehsenfeld, F. C.: A chemical ionization mass spectrometry technique for airborne
539 measurements of ammonia, *J. Geophys. Res.-Atmos.*, 112, D10S02, doi:10.1029/2006JD007589, 2007.

540
541 Nowak, J. B., Neuman, J. A., Bahreini, R., Brock, C. A., Middlebrook, A. M., Wollny, A. G., Holloway, J. S.,
542 Peischl, J., Ryerson, T. B., and Fehsenfeld, F. C.: Airborne observations of ammonia and ammonium nitrate
543 formation over Houston, Texas, *J. Geophys. Res.-Atmos.*, 115, D22 304, doi:10.1029/2010JD014195, 2010.

544
545 Rodgers, Clive D. *Inverse methods for atmospheric sounding: theory and practice*. Vol. 2. Singapore: World
546 scientific, 2000.

547
548 Rodhe, H., Dentener, F., & Schulz, M. (2002). The global distribution of acidifying wet deposition. *Environmental*
549 *Science & Technology*, 36(20), 4382-4388.

550
551 Rothman, L. S., I. E. Gordon, Y. Babikov, A. Barbe, D. Chris Benner, P. F. Bernath, Manfred Birk et al. "The
552 HITRAN2012 molecular spectroscopic database." *Journal of Quantitative Spectroscopy and Radiative*
553 *Transfer* 130 (2013): 4-50.
554
555 Paton-Walsh, C., Jones, N. B., Wilson, S. R., Haverd, V., Meier, A., Griffith, D. W., and Rinsland, C. P. (2005).
556 Measurements of trace gas emissions from Australian forest fires and correlations with coincident measurements
557 of aerosol optical depth. *Journal of Geophysical Research: Atmospheres (1984–2012)*, 110(D24).
558
559 Paulot, F., D. J. Jacob, R. W. Pinder, J. O. Bash, K. Travis, and D. K. Henze (2014), Ammonia emissions in the
560 United States, European Union, and China derived by high resolution inversion of ammonium wet deposition
561 data: Interpretation with a new agricultural emissions inventory (MASAGE NH3), *J. Geophys. Res.-Atmos.*,
562 *119*(7), 4343– 4364, doi:10.1002/2013JD021130.
563
564 Pope, III, C. A., Ezzati, M., and Dockery, D. W.: Fine-Particulate Air Pollution and Life Expectancy in the United
565 States, *N. Engl. J. Med.*, 360, 376–386, doi:{10.1056/NEJMsa0805646}, 2009.
566
567 Pougatchev, N. S., Connor, B. J., & Rinsland, C. P. (1995). Infrared measurements of the ozone vertical
568 distribution above Kitt Peak. *Journal of Geophysical Research: Atmospheres (1984–2012)*, 100(D8), 16689-
569 16697.
570
571 Pouliot, G., T. Pierce, H. D. van der Gon, M. Schaap, M. Moran, and U. Nopmongcol (2012), Comparing emission
572 inventories and model-ready emission datasets between Europe and North America for the AQMEII project,
573 *Atmos. Environ.*, 53(0), 4– 14, doi:10.1016/j.atmosenv.2011.12.041.
574
575 Puchalski, M. A., M. E. Sather, J. T. Walker, C. M. Lehmann, D. A. Gay, J. Mathew, and W. P. Robarge (2011),
576 Passive ammonia monitoring in the United States: Comparing three different sampling devices, *J. Environ. Monit.*,
577 *13*(11), 3156–3167, doi:10.1039/c1em10553a.
578
579 Rao, K.N., and A. Weber, Spectroscopy of the Earth's Atmosphere and Interstellar Medium, Academic, San Diego,
580 Calif., 1992

581 Reay, D. S., Dentener, F., Smith, P., Grace, J., & Feely, R. A. (2008). Global nitrogen deposition and carbon
582 sinks. *Nature Geoscience*, 1(7), 430-437.

583 Rodhe, Henning, Frank Dentener, and Michael Schulz. "The global distribution of acidifying wet
584 deposition." *Environmental Science & Technology* 36.20 (2002): 4382-4388.

585 Rothman, L. S., Gordon, I. E., Babikov, Y., Barbe, A., Benner, D. C., & Bernath, P. F. (2013). The HITRAN
586 database: 2012 edition. *J Quant Spectrosc Radiat Transfer*.
587
588 Rodgers, C. D., & Connor, B. J. (2003). Intercomparison of remote sounding instruments. *Journal of Geophysical*
589 *Research: Atmospheres (1984–2012)*, 108(D3).
590
591 Schaap, M., van Loon, M., ten Brink, H. M., Dentener, F. J., and Builtjes, P. J. H.: Secondary inorganic aerosol
592 simulations for Europe with special attention to nitrate, *Atmos. Chem. Phys.*, 4, 857-874, doi:10.5194/acp-4-857-
593 2004, 2004
594
595 Shephard, M. W., Cady-Pereira, K. E., Luo, M., Henze, D. K., Pinder, R. W., Walker, J. T., Rinsland, C. P.,
596 Bash, J. O., Zhu, L., Payne, V. H., and Clarisse, L.: TES ammonia retrieval strategy and global observations of
597 the spatial and seasonal variability of ammonia, *Atmos. Chem. Phys.*, 11, 10743-10763, doi:10.5194/acp-11-
598 10743-2011, 2011.

599 Shephard, M. W. and Cady-Pereira, K. E.: Cross-track Infrared Sounder (CrIS) satellite observations of
600 tropospheric ammonia, *Atmos. Meas. Tech.*, 8, 1323-1336, doi:10.5194/amt-8-1323-2015, 2015**b**.

601 [Shephard, M. W., McLinden, C. A., Cady-Pereira, K. E., Luo, M., Moussa, S. G., Leithead, A., Liggio, J., Staebler,](#)
602 [R. M., Akingunola, A., Makar, P., Lehr, P., Zhang, J., Henze, D. K., Millet, D. B., Bash, J. O., Zhu, L., Wells, K.](#)
603 [C., Capps, S. L., Chaliyakunnel, S., Gordon, M., Hayden, K., Brook, J. R., Wolde, M., and Li, S.-M.: Tropospheric](#)
604 [Emission Spectrometer \(TES\) satellite validations of ammonia, methanol, formic acid, and carbon monoxide over](#)
605 [the Canadian oil sands, Atmos. Meas. Tech. Discuss.](#), 8, 9503-9563, doi:10.5194/amt-8-9503-2015, 2015a.

606 Skjøth, C. A., Geels, C., Berge, H., Gyldenkerne, S., Fagerli, H., Ellermann, T., Frohn, L. M., Christensen, J.,
607 Hansen, K. M., Hansen, K., and Hertel, O.: Spatial and temporal variations in ammonia emissions – a freely
608 accessible model code for Europe, *Atmos. Chem. Phys.*, 11, 5221–5236, doi:10.5194/acp-11-5221-2011, 2011.

609 Sussmann, R., Borsdorff, T., Rettinger, M., Camy-Peyret, C., Demoulin, P., Duchatelet, P., Mahieu, E., and
610 Servais, C.: Technical Note: Harmonized retrieval of column-integrated atmospheric water vapour from the FTIR
611 network – first examples for long-term records and station trends, *Atmos. Chem. Phys.*, 9, 8987–8999, 2009.
612

613 Sutton, M. A., et al. (2013), Towards a climate-dependent paradigm of ammonia emission and deposition, *Philos.*
614 *Trans. R. Soc. London, Ser. B*, 368(1621), 20130166, doi:10.1098/rstb.2013.0166.
615

616 Thijsse, T. R., Duyzer, J. H., Verhagen, H. L. M., Wyers, G. P., Wayers, A., and Möls, J. J.: Measurement of
617 ambient ammonia with diffusion tube samplers, *Atmos. Environ.*, 32, 333–337, 1998.
618

619 Thomas, R. M., Trebs, I., Otjes, R., Jongejan, P. A. C., ten Brink, H., Phillips, G., Kortner, M., Meixner, F. X.,
620 and Nemitz, E.: An automated analyzer to measure surface-atmosphere exchange fluxes of water soluble inorganic
621 aerosol compounds and reactive trace gases, *Environ. Sci. Technol.*, 43, 1412–1418, 2009.
622

623 Toon, G. C., Blavier, J.-F., Sen, B., Margitan, J. J., Webster, C. R., Max, R. D., Fahey, D. W., Gao, R., DelNegro,
624 L., Proffitt, M., Elkins, J., Romashkin, P. A., Hurst, D. F., Oltmans, S., Atlas, E., Schauffler, S., Flocke, F., Bui,
625 T. P., Stimpfle, R. M., Bonne, G. P., Voss, P. B., and Cohen, R. C.: Comparison of MkIV balloon and ER-2
626 aircraft measurements of atmospheric trace gases, *J. Geophys. Res.*, 104, 26 779–26 790, 1999.
627

628 Van Damme, M., Clarisse, L., Heald, C. L., Hurtmans, D., Ngadi, Y., Clerbaux, C., Dolman, A. J., Erisman, J. W.,
629 and Coheur, P. F.: Global distributions, time series and error characterization of atmospheric ammonia (NH₃) from
630 IASI satellite observations, *Atmos. Chem. Phys.*, 14, 2905–2922, doi:10.5194/acp-14-2905-2014, 2014a.

631 Van Damme, M., R. J. Wichink Kruit, M. Schaap, L. Clarisse, C. Clerbaux, P.-F. Coheur, E. Dammers, A. J.
632 Dolman, and J. W. Erisman, Evaluating 4 years of atmospheric ammonia (NH₃) over Europe using IASI satellite
633 observations and LOTOS-EUROS model results, *J. Geophys. Res. Atmos.*, 119, 9549–9566,
634 doi:10.1002/2014JD021911, 2014b

635 Van Damme, M., Clarisse, L., Dammers, E., Liu, X., Nowak, J. B., Clerbaux, C., Flechard, C. R., Galy-Lacaux, C.,
636 Xu, W., Neuman, J. A., Tang, Y. S., Sutton, M. A., Erisman, J. W., and Coheur, P. F.: Towards validation of
637 ammonia (NH₃) measurements from the IASI satellite, *Atmos. Meas. Tech. Discuss.*, 7, 12125–12172,
638 doi:10.5194/amt-7-12125-2014, 2014c

639 Van Damme, M., Erisman, J. W., Clarisse, L., Dammers, E., Whitburn, S., Clerbaux, C., Dolman, A. J., and
640 Coheur, P. F., Worldwide spatiotemporal atmospheric ammonia (NH₃) variability revealed by satellite, *Geophys.*
641 *Research. Let.* (in revision), 2015.
642

643 Van Putten, E. M., Mennen, M. G., Regts, T., and Uiterwijk, J. W.: Performance study of four automatic ammonia
644 monitors under controlled conditions, report 723101004, RIVM, 1994
645

646 Vigouroux, C., Stavrakou, T., Whaley, C., Dils, B., Dufлот, V., Hermans, C., Kumps, N., Metzger, J.-M.,
647 Scolas, F., Vanhaelewyn, G., Müller, J.-F., Jones, D. B. A., Li, Q., and De Mazière, M.: FTIR time-series of
648 biomass burning products (HCN, C₂H₆, C₂H₂, CH₃OH, and HCOOH) at Reunion Island (21° S, 55° E) and
649 comparisons with model data, *Atmos. Chem. Phys.*, 12, 10367–10385, doi:10.5194/acp-12-10367-2012, 2012.

650 Vigouroux, 2013, EGU, Ground-based FTIR measurements of NH₃ total columns and comparison with IASI data

651 Vitousek, P. M., Aber, J., Howarth, R. W., Likens, G. E., Matson, P. A., Schindler, D. W., Schlesinger, W. H., &
652 Tilman, G. D. (1997). *Human alteration of the global nitrogen cycle: causes and consequences*. Washington, DC,
653 US: Ecological Society of America.

654 Volten, H., Bergwerff, J. B., Haaima, M., Lolkema, D. E., Berkhout, A. J. C., van der Hoff, G. R., Potma, C. J. M.,
655 Wichink Kruit, R. J., van Pul, W. A. J., and Swart, D. P. J.: Two instruments based on differential optical
656 absorption spectroscopy (DOAS) to measure accurate ammonia concentrations in the atmosphere, *Atmos. Meas.*
657 *Tech.*, 5, 413–427, doi:10.5194/amt-5-413-2012, 2012.

658 Whitburn, S., Van Damme, M., Kaiser, J. W., van der Werf, G. R., Turquety, S., Hurtmans, D., Clarisse, L.,
659 Clerbaux, C., Coheur, P. F. (2015). Ammonia emissions in tropical biomass burning regions: Comparison between
660 satellitederived emissions and bottom-up fire inventories, *Atmospheric Environment* (2015),
661 <http://dx.doi.org/10.1016/j.atmosenv.2015.03.015>

662 [Wood, S. W.: Validation of version 5.20 ILAS HNO₃, CH₄, N₂O, O₃, and NO₂ using ground-based](#)
663 [measurements at Arrival Heights and Kiruna, *J. Geophys. Res.*, 107\(D24\), 8208, doi:10.1029/2001JD000581,](#)
664 [2002.](#)

666 [Yokelson, R. J., Susott, R., Ward, D. E., Reardon, J. and Griffith, D. W. T.: Emissions from smoldering](#)
667 [combustion of biomass measured by open-path Fourier transform infrared spectroscopy, *J. Geophys. Res.*,](#)
668 [102\(D15\), 18865, doi:10.1029/97JD00852, 1997.](#)

669 [Yokelson, R., Urbanski, S., Atlas, E., Toohey, D., Alvarado, E., Crouse, J., Wennberg, P., Fisher, M., Wold, C.,](#)
670 [Campos, T., Adachi, K., Buseck, P. R. and Hao, W. M.: Emissions from forest fires near Mexico City, *Atmos.*](#)
671 [Chem. Phys. Discuss., 7\(3\), 6687–6718, doi:10.5194/acpd-7-6687-2007, 2007.](#)

672 ▲

Formatted: English (United States)

673 Zander, R., Mahieu, E., Demoulin, P., Duchatelet, P., Roland, G., Servais, C., De Mazière, M., Reimann, S.,
674 and Rinsland, C.P.: Our changing atmosphere: Evidence based on long-term infrared solar observations at the
675 Jungfraujoch since 1950, *Sci. Total Environ.*, 391, 184-195, 2008.

676 [Zhu, L., Henze, D. K., Cady-Pereira, K. E., Shephard, M. W., Luo, M., Pinder, R. W., Bash, J. O. and Jeong, G.](#)
677 [R.: Constraining U.S. ammonia emissions using TES remote sensing observations and the GEOS-Chem adjoint](#)
678 [model, *J. Geophys. Res. Atmos.*, 118\(8\), 3355–3368, doi:10.1002/jgrd.50166, 2013.](#)

680

681 **Tables****Table 1** FTIR stations used in the analysis. The location, longitude, latitude and altitude are given for each station as well as the instrument used for the measurements. Some station specifics are given in the last column.

Station	Location	Longitude	Latitude	Altitude (m.a.s.l.)	Instrument	Station specifics
Bremen	Germany	8.85E	53.10N	27	Bruker 125 HR	City, fertilizers, livestock
Lauder	New Zealand	169.68E	45.04S	370	Bruker 120 HR	Fertilizers, livestock
Reunion	Indian Ocean	55.5E	20.90S	85	Bruker 120 M	Fertilizers, fires
Jungfrauoch	Switzerland	7.98E	46.55N	3580	Bruker 120 HR	High altitude, no large sources

682

Table 2 Micro windows used in the NH₃ retrieval at the four stations.

Stations	Micro window	Spectral range (cm ⁻¹)	Interfering species (Profile retrieved species in bold)	SNR Signal-to-noise ratio (SNR)
Bremen and Lauder	MW1	930.32-931.32	NH₃, H₂O, O₃ , CO ₂ , N ₂ O, HNO ₃ , SF ₆ , CFC-12, solar lines	Bremen – Real SNR mean value of 450
	MW2	966.97-967.68	NH₃, H₂O, O₃ , CO ₂ , N ₂ O, HNO ₃ , solar lines	Lauder – Real SNR mean value of 250
Reunion	MW1	929.4-931.4	NH₃, H₂O, O₃ , CO ₂ , N ₂ O, HNO ₃ , SF ₆ , CFC-12	Reunion – Real SNR mean value of 365
	MW2	962.1-970.0	NH₃, H₂O, O₃ , CO ₂ , N ₂ O, HNO ₃ , HDO, ⁶⁸⁶ O ₃ , solar lines	
Jungfrauoch	MW1	929.4-931.4	NH₃, H₂O, O₃ , CO ₂ , N ₂ O, HNO ₃ , SF ₆ , CFC-12	
	MW2	962.1-970.0	NH₃, H₂O, O₃ , CO ₂ , N ₂ O, HDO, ⁶⁸⁶ O ₃ , solar lines	Jungfrauoch – Fixed at 250

683

684 **Table 3** Random and Systematic uncertainties used in the error calculation

Version (Stations)	SFIT 4 (Bremen, Lauder, Reunion)		Version (Stations)	SFIT 2 (Jungfrauoch)	
Parameter	Random uncertainty	Systematic uncertainty	Parameter	Random uncertainty	Systematic uncertainty
Temperature	2 K troposphere 5 K stratosphere	2 K troposphere 5 K stratosphere	Temperature	1.5 K 0-20km 2.0 K 20-30km 5.0 K 30km -	
Solar line shift	0.005 cm ⁻¹	0.005 cm ⁻¹	Line intensity		20.0%
Solar line strength	0.1 %	0.1 %	Line T broadening		10.0%
Solar zenith angle	0.01 Degrees	0.01 Degrees	Line P broadening		10.0%
Phase	0.001 Rad	0.001 Rad	Interfering species		HITRAN2012: varies
Zero level	0.01	0.01	Instrumental Line Shape (ILS)		10%
Background curvature		0.001 cm ⁻²	Influence a priori profiles	Calculated	
Field of view		0.001	Solar Zenith Angle (SZA)	0.2 degrees	
Line intensity		20.0%			
Line T broadening		10.0%			

Line P broadening		10.0%			
Interfering species	HITRAN2012: varies				

Table 4 Mean random and systematic errors for each of the individual NH₃ retrieval parameters. The table is split into two sections to cover both the error calculation using SFIT4 (Bremen, Lauder, Reunion) and SFIT2 (Jungfraujoch). At the bottom the errors are summarized into total mean errors for each of the stations.

Station	Bremen		Lauder		Reunion		Jungfraujoch		
Parameter	Mean Random Error (%)	Mean Systematic Error (%)	Mean Random Error (%)	Mean Systematic Error (%)	Mean Random Error (%)	Mean Systematic Error (%)	Parameter	Mean Random Error (%)	Mean Systematic Error (%)
Temperature	4.9	4.9	3.6	3.6	2.7	2.9	Temperature	15.2	
Solar zenith angle	1.6	1.6					Solar zenith angle	1.9	
Phase	1.0	1.0	1.1	1.1			Instrumental lineshape		1.4
Zero level	5.0	5.0	6.8	6.8					
Measurement noise	4.5		8.4		10.9		Measurement noise	18.2	
Interfering Species	1.3		2.4		0.9	8.7 (H ₂ O line pressure broadening)	Interfering species		1.4
Retrieval parameters	0.1		0.1				Model parameters	1.4	
Background curvature		1.1		1.2		0.3	Forward model		1.0
Smoothing error		2.8		8.1	10.3		Smoothing	5.4	
Spectroscopy		21.0		22.7		17.8	Spectroscopy		20.1
							NH ₃ a priori		6.1
							Influence a priori profiles (H ₂ O & HDO)	6.6	
Subtotal error	9.1	23.5	12.0	27.0	15.3	20.0	Subtotal error	25.3	23.1
Total error	25.8		30.2		25.2		Total	34.2	

Table 5 Statistics of the NH₃ columns. (Nr: number of data points, DOFS: Degree of Freedom for Signal, Mean \pm the error of the mean, RMS: Root Mean Square). Total columns are given in 1e15 molecules NH₃ cm⁻².

Station	Nr	Mean DOFS	Mean (molecules x 1e15)	Median (molecules x 1e15)	RMS (molecules x 1e15)
Bremen	554	1.9	13.75 \pm 4.24	9.51	20.22
Lauder	2412	1.4	4.17 \pm 1.40	2.85	5.95
Reunion	1262	1.0	0.80 \pm 0.54	0.56	1.14
Jungfraujoch	2702	1.0	0.18 \pm 0.07	0.15	0.22

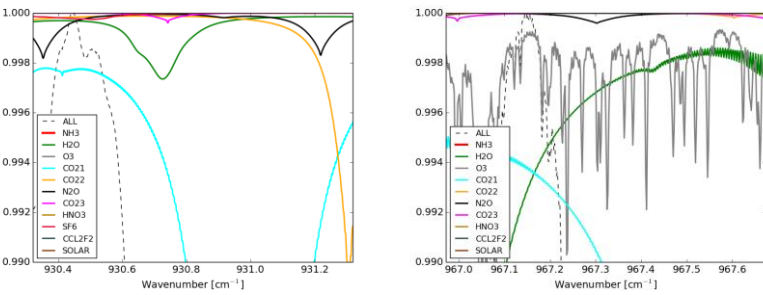
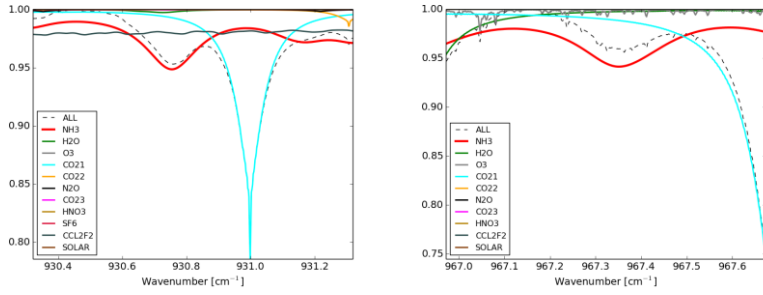
685

686

687

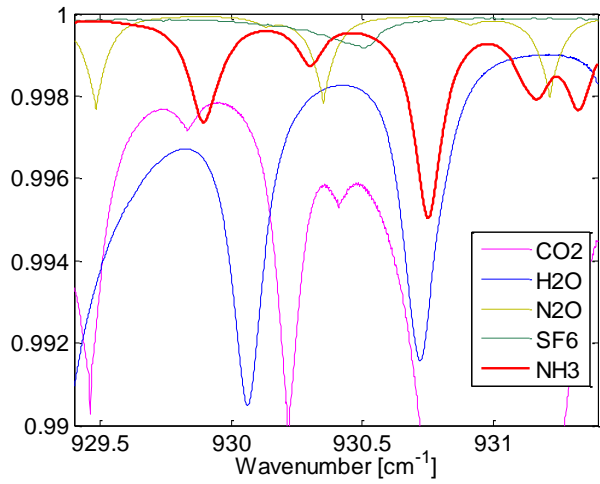
688

689 **Figures**

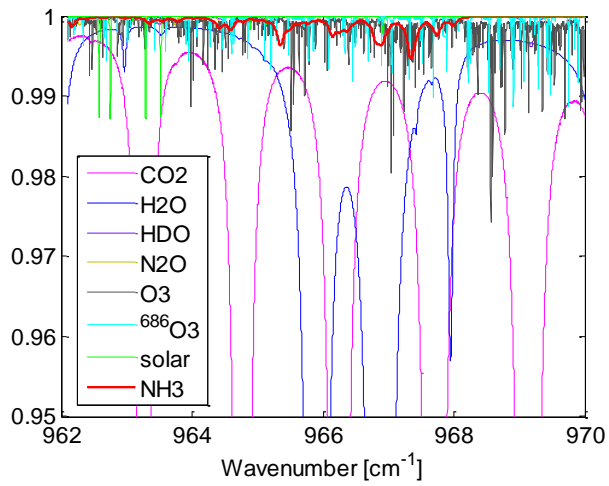


692 Figure 1 Calculated spectrum for both spectral windows measured with the 125HR in Bremen on the 19th of
693 April 2010 at 09:59 (UTC) corresponding to a total column of 18.83×10^{15} molecules cm^{-2} . The top two panels
694 show the individual contributions of the different species in the first (MW1) and second (MW2) spectral
695 windows. The second row show the same calculated spectra but now with the y-axis scaled to show the minor
696 interfering species.

697



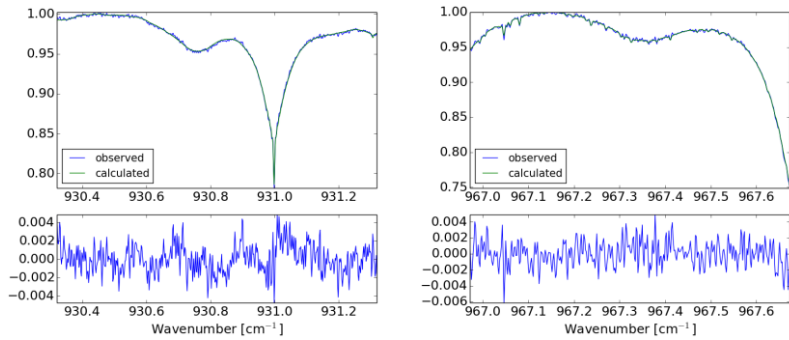
698



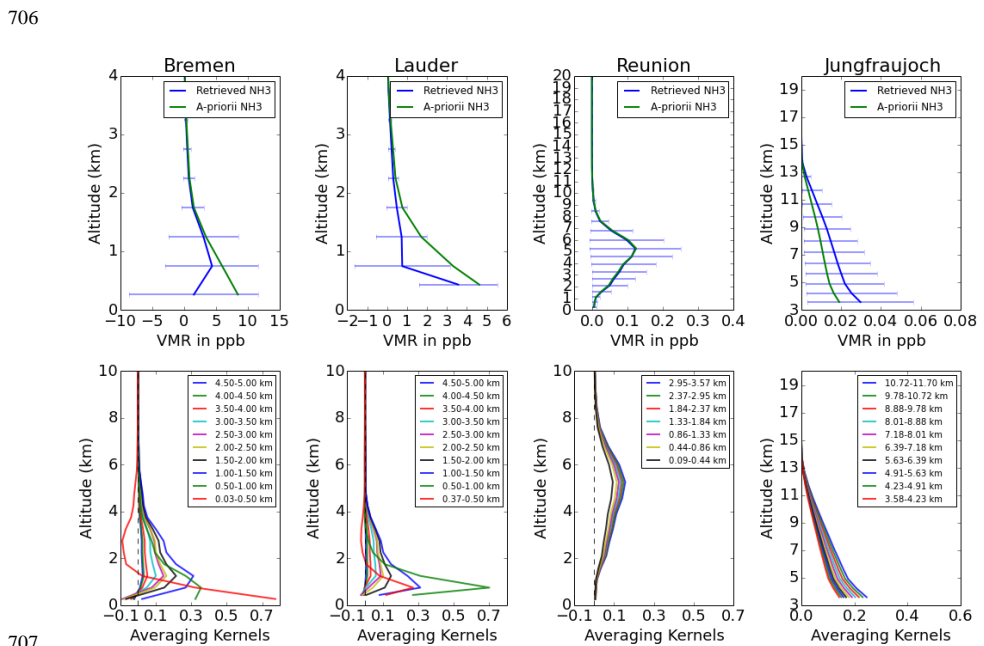
699

Figure 2 Example of a synthetic atmospheric spectrum for both spectral windows at Reunion Island, computed for the 5th June 2011 and a total column of 1.07E15 molecules cm⁻². The top panel shows the individual contributions of the main species in the first spectral window. The bottom panel shows the second spectral window.

700



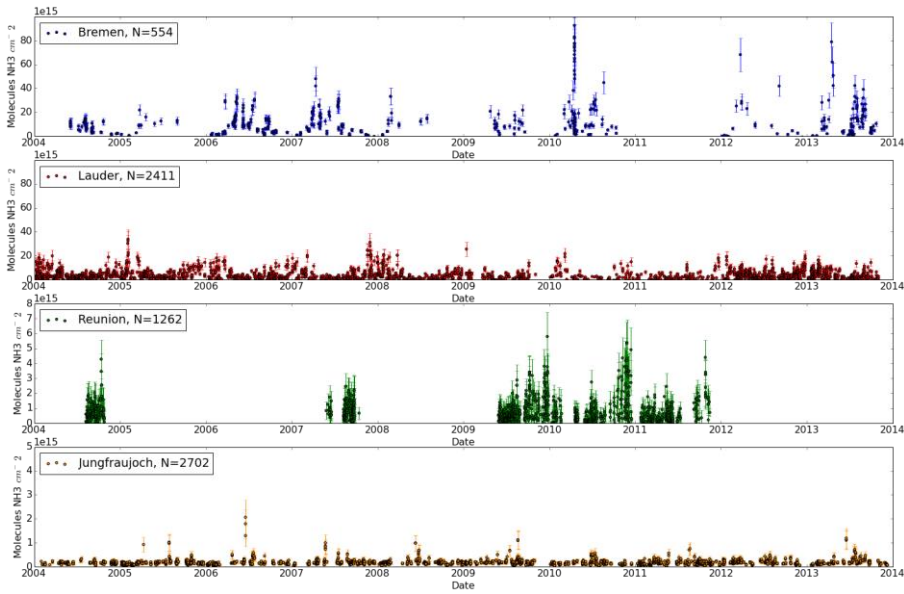
701
 702 Figure 3 Measured and calculated spectrum for both spectral windows measured with the 125HR in Bremen on
 703 the 19th of April 2010 at 09:59 (UTC) corresponding to a total column of 18.83e15 molecules $\text{NH}_3 \text{ cm}^{-2}$. The top
 704 two panels show the observed (blue line) and calculated (green line) spectra for MW1 (left) and MW2 (right). The
 705 bottom two figures show the residuals of the fits in both spectral windows.



707
 708 Figure 4 Top panels: the retrieved NH_3 profile (blue) and the a-priori profile (green) in order from left to right:
 709 Bremen (Left), Lauder (Left middle), Reunion island (right middle) and Jungfraujoch (right). Horizontal lines
 710 indicate the standard deviation in all observations for each layer. Bottom panels: the normalized averaging kernel
 711 for each of the stations.

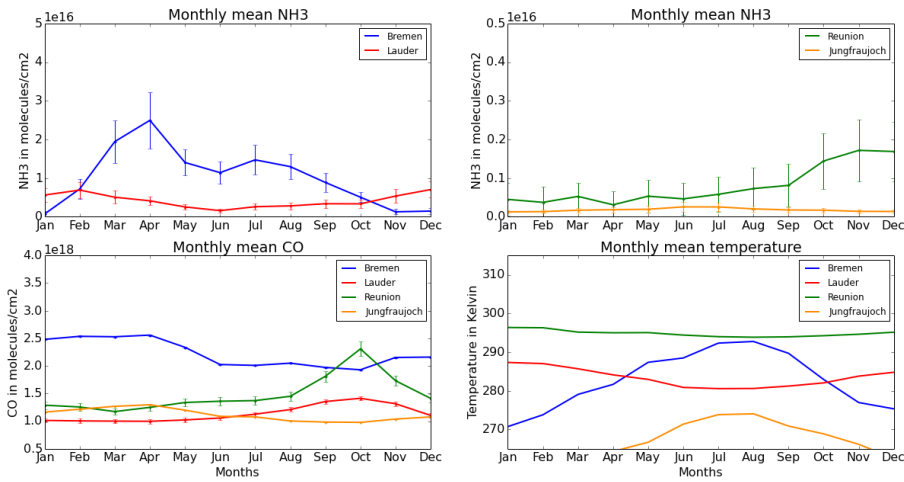
712

713
714



715
716
717
718
719

Figure 5 Time series of retrieved NH_3 columns (in molecules $\text{NH}_3 \text{ cm}^{-2}$). From top to bottom the figure shows the Bremen (blue), Lauder (red), Reunion (green) and Jungfraujoch (yellow) total columns. The bars reflect the errors on the individual observations.



720

Figure 6 2004-2013 monthly averaged columns for NH_3 , CO and temperature. The top two panels show the monthly NH_3 column concentrations (molecules $\text{NH}_3 \text{ cm}^{-2}$) for each of the four stations. Vertical lines indicate the

mean monthly error. The bottom two panels show additional column concentrations of CO (bottom, left) and temperature (bottom, right).

